Available online at www.sciencedirect.com
ScienceDirect
Trans. Nonferrous Met. Soc. China 28(2018) 912−919
Transactions of Nonferrous Metals Society of China
www.tnmsc.cn

Effect of predeformation on globularization of Ti−5Al−2Sn−2Zr−4Mo−4Cr during annealing

Lian LI, Miao-quan LI

School of Materials Science and Engineering, Northwestern Polytechnical University, Xi'an 710072, China

Received 22 November 2016; accepted 28 April 2017

Abstract: The microstructure evolution during annealing of Ti−5Al−2Sn−2Zr−4Mo−4Cr alloy was investigated. The results show that for the alloy compressed at 810 °C and 1.0 s^{-1}, deformation amount (height reduction) 20% and 50% and annealed at 810 °C, thermal grooving by penetration of β phase is sufficient during the first 20 min annealing, resulting in a sharp increase in globularization fraction. The globularization fraction continuously increases with the increase of annealing time, and a height reduction of 50% leads to a near globular microstructure after annealing for 4 h. For the alloy with deformation amount of 50% by compressing at 810 °C, 0.01 s^{-1}, and then annealed at 810 °C, thermal grooving is limited during the first 20 min of annealing and large quantities of high-angle grain boundaries (HABs) remain. With long time annealing, the chain-like α grains are developed due to the HABs, termination migration and Ostwald ripening. The present results suggest that a higher strain rate and a larger height reduction are necessary before annealing to achieve a globular microstructure of Ti−5Al−2Sn−2Zr−4Mo−4Cr.
Key words: Ti−5Al−2Sn−2Zr−4Mo−4Cr alloy; annealing; thermal grooving; globularization; high-angle grain boundaries

1 Introduction

Titanium alloys have been widely used in aviation, aerospace, marine and other specialty supplications due to their high specific strength and good corrosion resistance [1,2]. It is well known that titanium alloys with lamellar α microstructure have good resistance to fracture but low ductility, while titanium alloys with globular α microstructure show better balance of strength and ductility which are more desirable for many service applications [3,4]. As a result, control of α morphology (such as lamellar, globular) in titanium alloys by a series of thermomechanical processing (TMP) steps was of great importance to meet the microstructure and mechanical properties requirements [5,6]. Among these steps, hot working in the α/β two-phase field was usually carried out so as to break down lamellar α into globular α [7−9]. Besides, subsequent annealing in the α/β two-phase field was performed to adjust the microstructure for final property requirement [10−12]. Regarding the great importance of globularization in controlling the mechanical properties of titanium alloys in industry, a wide variety of investigations have been carried out. The globularization kinetics both in the hot working of titanium alloys [8,13] was well established so as to predict the microstructure evolution. Besides, the mechanisms controlling globularization during hot working were proposed for the typical α/β two-phase titanium alloys. SEMIATIN [11] and ROY et al [14] showed that the boundary splitting was responsible for the fragmentation of α lamellae during hot working. STEFANSSON and SEMIATIN [15] suggested the fragmentation of α lamellae by boundary splitting in the initial stage of static globularization, while microstructural coarsening characterized the microstructure evolution as the annealing time increased.

Our previous work [16] showed that the strain rate and height reduction played an important role both in α and β phases evolution of Ti−5Al−2Sn−2Zr−4Mo−4Cr alloy with a colony α microstructure. The globularization of α lamellae was enhanced with the increase of height reduction and the decrease of strain rate. Besides, low-angle boundaries (LABs) and high-angle boundaries (HABs) occurred after compression at 810°C, while more HABs occurred in the β phase at a strain rate of 1.0 s^{-1} than that at a strain rate of 0.01 s^{-1}. The dislocation substructures (LABs and HABs) may drive

Foundation item: Project (51275416) supported by the National Natural Science Foundation of China; Project (KP201513) supported by the Fund of the State Key Laboratory of Solidification Processing in NWPU, China
Corresponding author: Miao-quan LI; Tel: +86-29-88460328; Fax: +86-29-88492642; E-mail: honeymli@nwpu.edu.cn
DOI: 10.1016/S1003-6326(18)64725-9

the thermal grooving in the early stage of annealing [11,12,15], which affected the final microstructure after annealing. However, the effect of predeformation on static globularization of Ti−5Al−2Sn−2Zr−4Mo−4Cr is still unclear, which prevents microstructure control of Ti−5Al−2Sn−2Zr−4Mo−4Cr to obtain the desired properties.

The present aim is to expand upon the previous work [16] to investigate the effect of predeformation on the globularization of Ti−5Al−2Sn−2Zr−4Mo−4Cr during annealing in the α/β two-phase field. To this end, the microstructure evolution during annealing of Ti−5Al−2Sn−2Zr−4Mo−4Cr specimens compressed at different strain rates and height reductions was investigated via scanning electron microscopy (SEM) and electron backscattered diffraction (EBSD) techniques. Besides, quantitative analysis of microstructure evolution during annealing (globularization fraction, length and thickness of α laths and/or grains) was carried out. The present results can provide guidance for achieving a globular microstructure of Ti−5Al−2Sn−2Zr−4Mo−4Cr by using predeformation and subsequent annealing in the α/β two-phase field.

2 Experimental

The Ti−5Al−2Sn−2Zr−4Mo−4Cr was supplied as a hot-forged bar consisting of ~16.3% (volume fraction) equiaxed primary α grains, ~8.0% elongated primary α grains and retained β phase (Fig. 1(a) in Ref. [17]). The measured composition (mass fraction) was 5.15% Al, 2.16% Sn, 2.09% Zr, 4.02% Mo, 4.01% Cr, 0.096% Fe, 0.009% C, 0.008% N, 0.006% H, 0.12% O and bal. Ti. The transus temperature of Ti and β phase (at which $\alpha+\beta\rightarrow\beta$) was approximately 900 °C. The as-received alloy bar was solution treated at 910 °C for 20 min followed by furnace cooling to room temperature to obtain a colony α microstructure (Fig. 1(b) in Ref. [17]).

Cylindrical specimens with 8.0 mm in diameter and 12.0 mm in height were axial sectioned from the heat-treated bar. Isothermal compression was carried out on a Gleeble−1500 simulator. Thermocouple was welded on the middle surface of Ti−5Al−2Sn−2Zr−4Mo−4Cr specimens to measure the actual deformation temperature, and graphite powder was put between the specimens and anvils so as to reduce the friction. The deformation conditions were 810 °C, 1.0 s^{-1}, 20% 50% (height reduction) and 810 °C, 0.01 s^{-1}, 50% (height reduction). The compressed specimens were annealed at 810 °C for 20 min, 1 h, 2 h and 4 h so as to investigate the effect of predeformation on globularization during annealing. After annealing, the specimens were air-cooled to room temperature. The axial sections in the central portion of annealed specimens were prepared to observe the microstructure evolution. The samples were mechanical polished and chemically etched with a solution of 10% HNO_3, 15% HF and 75% H_2O (volume fraction) and examined on a TESCAN VEGA3 LMU SEM. The globularization was taken to be an α phase morphology with an aspect ratio ($k=l/b$, l and b respectively denote the length and thickness of α laths and/or grains) of less than 3:1 using the Image-Pro Plus 6.0 software. EBSD observation was carried out to further clarify the microstructure evolution mechanisms. The specimens for EBSD examination were prepared as that in the previous study [16] and observed on a TESCAN MIRA3 XMU SEM equipped with a NordlysMax EBSD detector.

3 Results and discussion

3.1 As-deformed microstructures

Figure 1 shows the microstructures of Ti−5Al−2Sn−2Zr−4Mo−4Cr isothermally compressed at 810 °C. After

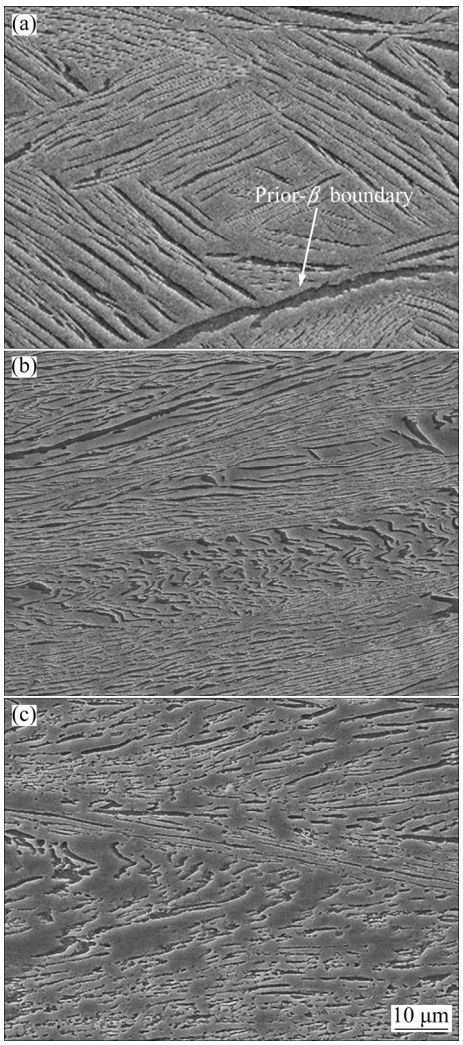

Fig. 1 Microstructures of Ti−5Al−2Sn−2Zr−4Mo−4Cr compressed at 810 °C, 1.0 s^{-1}, 20% (a), 810 °C, 1.0 s^{-1}, 50% (b) and 810 °C, 0.01 s^{-1}, 50% (c)

compressing at 810 °C, 1.0 s^{-1}, 20%, most of α phase presents a lamellar morphology, and the prior β boundary (indicated by the white arrow) can be detected, as shown in Fig. 1(a). After compressing at 810 °C, 1.0 s^{-1} and 50%, the α phase is mainly characterized with short α laths (Fig. 1(b)), and the globularization fraction is higher than that at a lower height reduction, as shown by the black and red arrows in Fig. 2(a). After being compressed at 810 °C, 0.01 s^{-1} and 50% (Fig. 1(c)), lots of globular α grains occur, and the globularization fraction is higher than that at higher strain rate, as shown by the blue arrow in Fig. 2(a). As a result, the length of α laths and/or grains at 810 °C, 0.01 s^{-1} and 50% is much shorter compared with that at 810 °C, 1.0 s^{-1}, 20% and 50%, as shown by the arrows in Fig. 2(b). The thickness values of α laths and/or grains at different strain rates and height reductions do not show much difference (indicated by the arrows in Fig. 2(c)). It is generally understood that boundary splitting is responsible for the globularization of α lamellae during hot working [11,14], in which penetration of β phase along HABs within α lamellae occurs. As a result, more globular α grains occur following compression at a larger height reduction and lower strain rate in which more HABs occur and penetration of β phase is sufficient.

3.2 As-annealed microstructures

Figure 3 shows the microstructures of alloys compressed at 810 °C, 1.0 s^{-1}, 20% and then annealed at 810 °C. As seen from Fig. 3(a), more globular α grains occur after annealing for 20 min compared with those of the as-compressed (Fig. 1(a)), leading to a sharp increase in globularization fraction (Fig. 2(a)) and decrease in length of α laths and/or grains (Fig. 2(b)). After long time annealing, more globular α grains occur while the globularization rate decreases, as shown in Fig. 2(a). In particular, the prior-β boundary still exists even after annealing for 1 h, as shown by the white arrow in Fig. 3(b). Besides, it should be mentioned that lots of long α laths can be detected in Fig. 3(b). The length of α laths and/or grains shows a more complicated variation after annealing for 20 min, and it keeps on decreasing after annealing for 1 h and then slightly increases with the increase of annealing time (Fig. 2(b)). Meanwhile, the thickness of α laths and/or grains continuously increases with the increase of annealing time, as shown in Fig. 2(c).

For the specimens compressed at 810 °C, 1.0 s^{-1}, 50% and then annealed at 810 °C, globularization is much more sufficient after annealing for 20 min (Fig. 4(a)) compared with that in Fig. 3(a). As seen from Fig. 4(a), only a few long α laths remain. As a consequence, the globularization fraction shows a more evident increase (Fig. 2(a)) and the length of α laths and/or grains rapidly decreases (Fig. 2(b)) after annealing for 20 min. After long time annealing, more globular α grains occur (Figs. 4(b) and (c)), and a near globular microstructure eventually occurs after annealing for 4 h (Fig. 4(d)). Moreover, the variation of globularization fraction, length and thickness of α laths

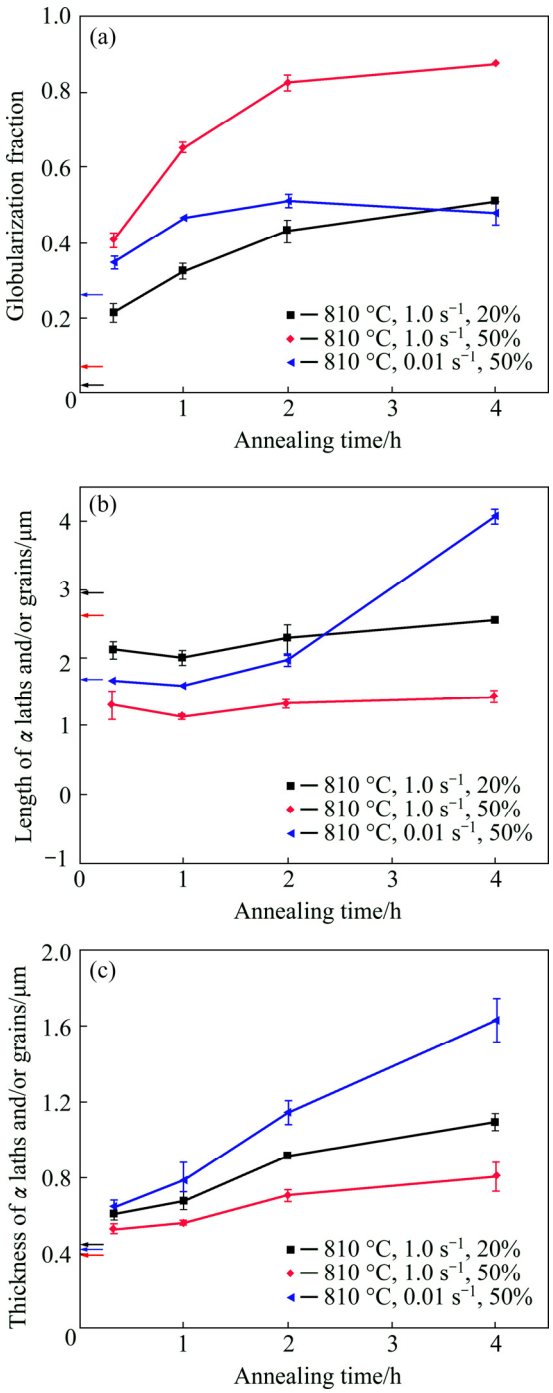

Fig. 2 Curves indicating globularization fraction (a), length (b) and thickness (c) of α laths and/or grains of Ti−5Al−2Sn−2Zr−4Mo−4Cr after annealing (Arrows in (a−c) respectively indicate globularization fraction, length and thickness of α laths and/or grains for as-compressed conditions)

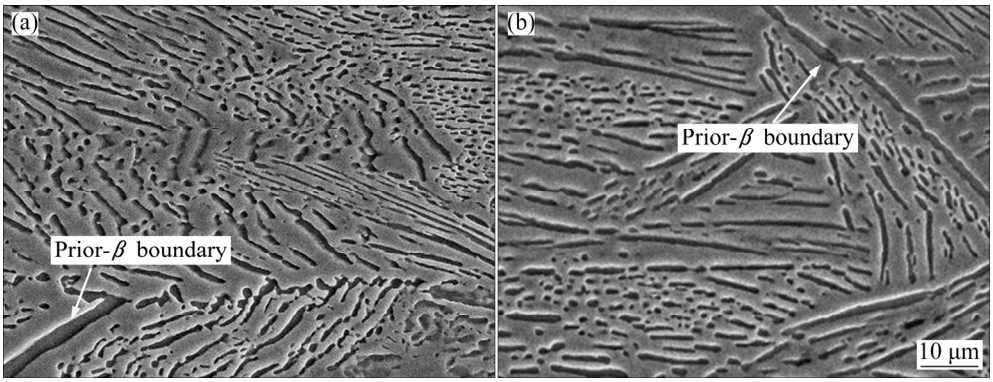

Fig. 3 Microstructures of Ti−5Al−2Sn−2Zr−4Mo−4Cr compressed at 810 °C, 1.0 s^{-1}, 20% and then annealed at 810 °C for 20 min (a) and 1 h (b)

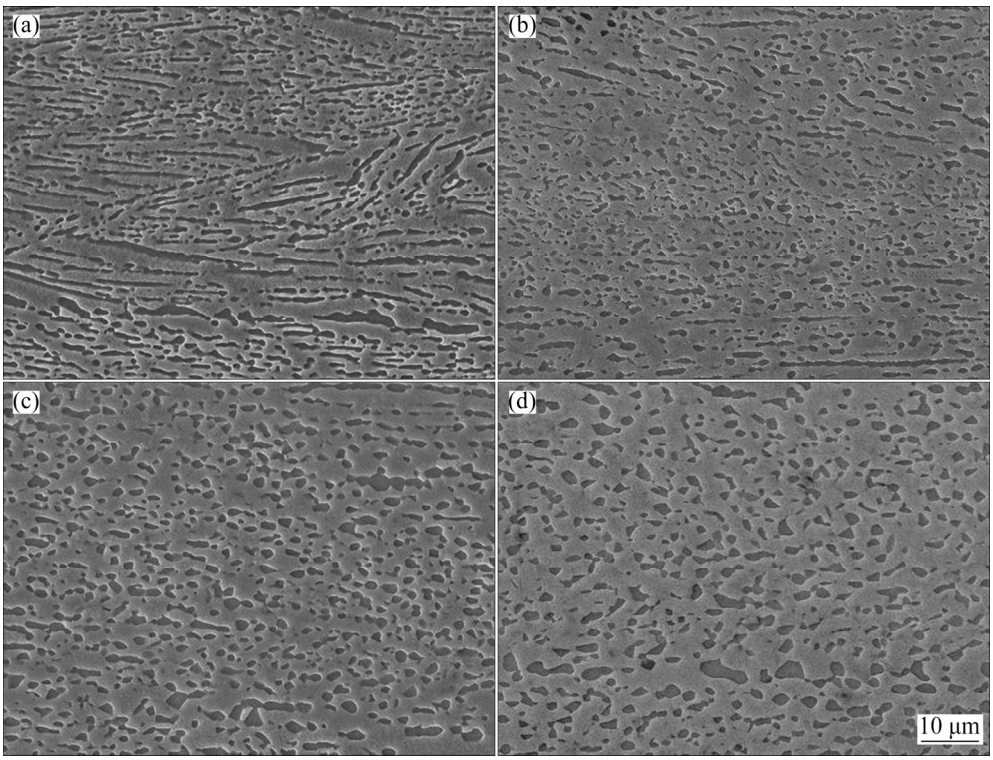

Fig. 4 Microstructures of Ti−5Al−2Sn−2Zr−4Mo−4Cr compressed at 810 °C, 1.0 s^{-1}, 50% and then annealed at 810 °C for 20 min (a), 1 h (b), 2 h (c) and 4 h (d)

and/or grains (Figs. 2(a)−(c)) generally shows similar trends with that of specimens compressed at 20% and then annealed.

Annealing the specimens (compressed at 810 °C, 0.01 s^{-1}, 50%) at 810 °C, it is interesting to find that the globularization fraction increases at annealing time from 20 min to 2 h and then decreases at annealing time of 2−4 h (Fig. 2(a)). Besides, the length of α laths and/or grains shows an initial decrease during the first 1 h of annealing and then sharply increases at annealing time of 2−4 h (Fig. 2(b)). These microstructure changes are quite different from those of specimens compressed at 1.0 s^{-1} and then annealed, which can be rationalized by the microstructure evolution in Fig. 5. Coalescence of adjacent α laths and/or grains occurs at annealing time of 2−4 h (indicated by the red arrows in Fig. 5(c)), contributing to the increase in the length of α laths and/or grains and the decrease in the globularization fraction. Meanwhile, the thickness presents a more evident increase at annealing time of 2−4 h compared with that of the specimens compressed at 810 °C, 1.0 s^{-1}, 20% and 50% and then annealed (Fig. 2(c)). Besides, it should be mentioned that α laths generally present a chain-like morphology following annealing for 2 and 4 h, as shown by the black arrows in Figs. 5(b) and (c).

3.3 Effect of predeformation on static globularization

Figure 6(a) shows the orientation evolution for α phase of Ti−5Al−2Sn−2Zr−4Mo−4Cr compressed at 810 °C, 1.0 s^{-1}, 50% and then annealed at 810 °C for

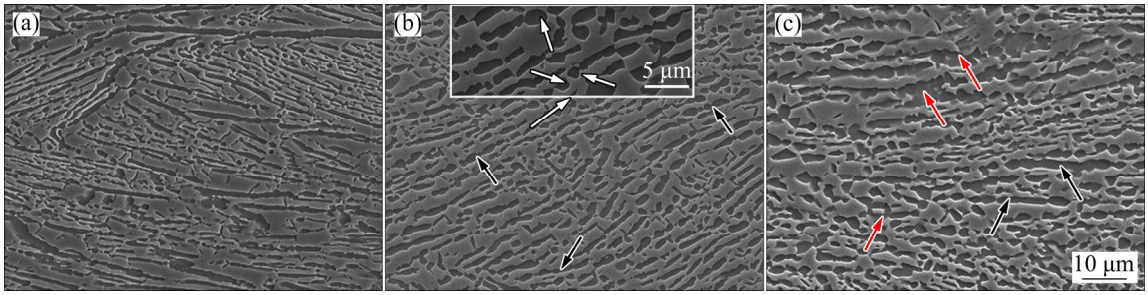

Fig. 5 Microstructures of Ti−5Al−2Sn−2Zr−4Mo−4Cr compressed at 810 °C, 0.01 s^{-1}, 50% and then annealed at 810 °C for 20 min (a), 2 h (b) and 4 h (c)

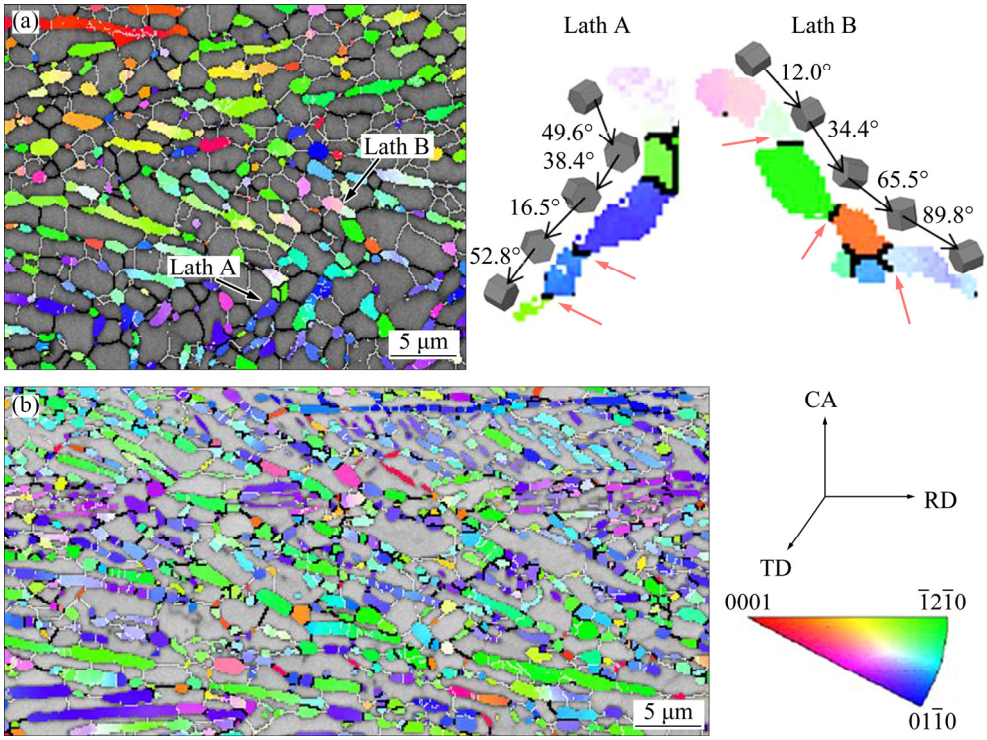

Fig. 6 Inverse pole figures (//compression axis (CA)) for α phase of Ti−5Al−2Sn−2Zr−4Mo−4Cr compressed at 810 °C, 1.0 s^{-1}, 50% and then annealed at 810 °C for 20 min (a) and compressed at 810 °C, 0.01 s^{-1}, 50% and then annealed at 810 °C for 20 min (b) (β phase is indicated in band contrast form. The black lines correspond to HABs with misorientation over 15° while white lines represent LABs with misorientation between 2° and 15°)

20 min. As seen from Fig. 6(a), the α phase is mainly composed of globular α grains and short α laths. Misorientation across α laths can be easily observed, and HABs are well developed in some α laths. However, for the specimen compressed at 810 °C, 0.01 s^{-1}, 50% and then annealed at 810 °C for 20 min (Fig. 6(b)), most of α phases still present a lamellar structure and large quantities of HABs exist. The grain boundary misorientation distribution for α phase in Figs. 6(a) and (b) is shown in Fig. 7(a). As seen from Fig. 7(a), the fraction of HABs for α phase in Fig. 6(b) is much higher than that in Fig. 6(a).

Taking a further investigation into the long α laths in Fig. 6(a), it can be concluded that pinch-off of α laths occurs by grooving along the HABs, similar to the case in laths A and B (indicated by the red arrows). The grooving process is highly associated with the intraphase α/α boundaries and penetration of β phase [11,18,19]. An initially semi-coherent boundary turns into high-energy non-coherent one after compression as reported in Refs. [20,21], in which HABs occur and provide sufficient driving force during subsequent annealing. As a result, it can be concluded that predeformation significantly affects the microstructure evolution during the early stage of annealing, which may affect further annealing at long time and final microstructure. In the following, schematic illustrations (Figs. 8 and 9) are shown for better understanding the effect of predeformation on static globularization of Ti−5Al−2Sn−2Zr−4Mo−4Cr.

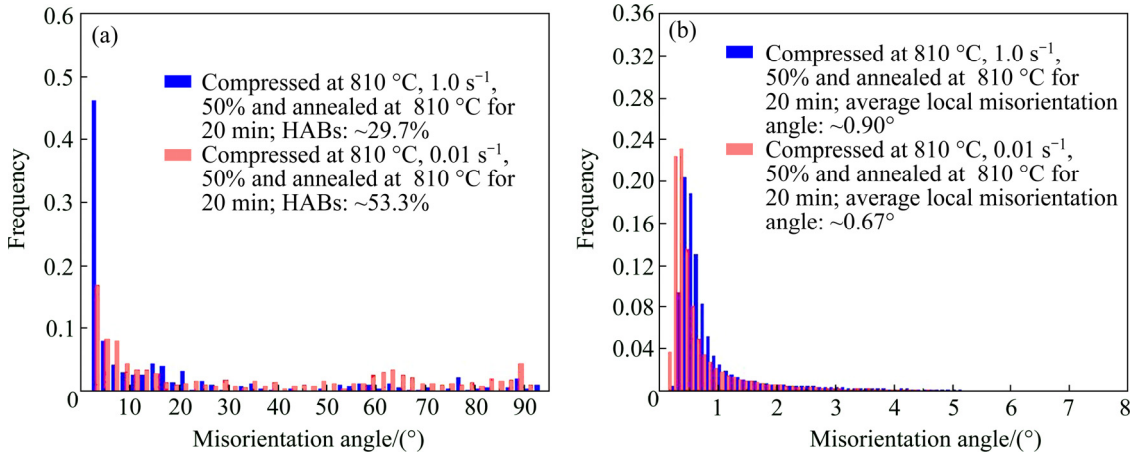

Fig. 7 Distribution of grain boundary misorientation for α phase (a) and local misorientation for β phase (b) of Ti−5Al−2Sn−2Zr−4Mo−4Cr

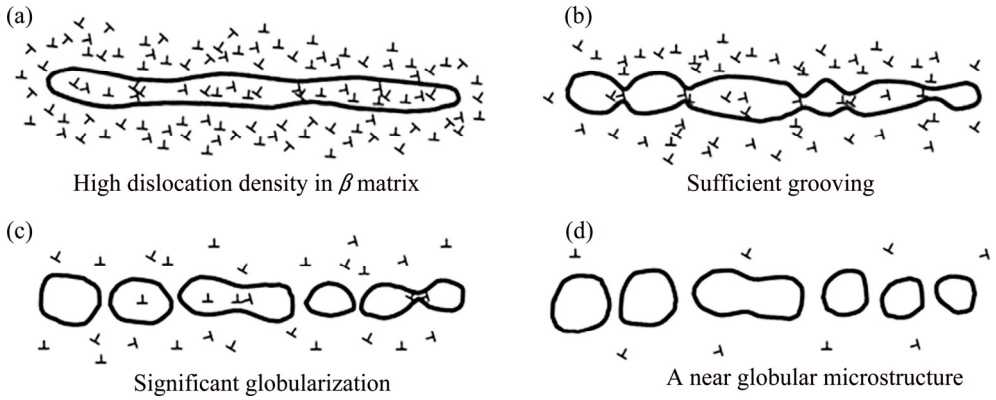

Fig. 8 Schematic illustration of microstructure evolution compressed at high strain rate and then annealed

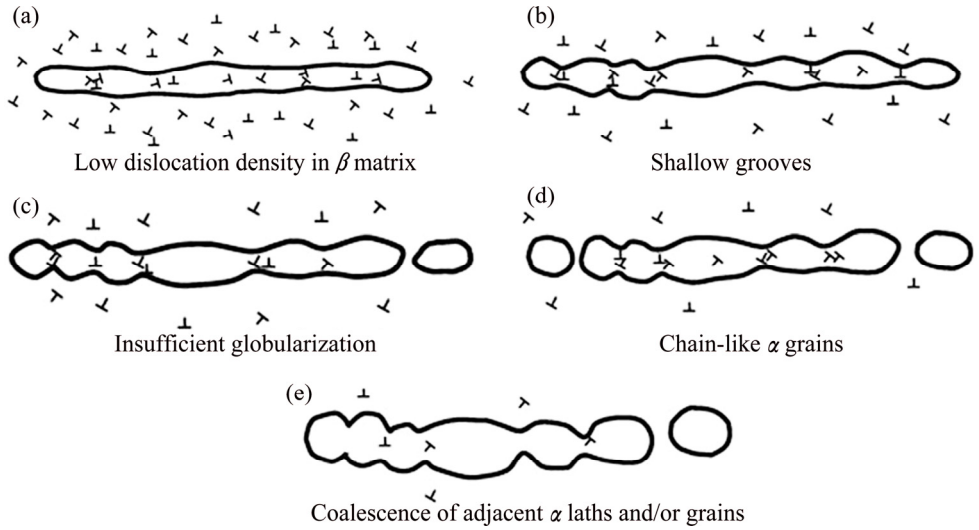

Fig. 9 Schematic illustration of microstructure evolution compressed at low strain rate and then annealed

As seen from Figs. 8(a) and 9(a), more dislocations remain in β matrix during the early stage of annealing after a higher strain rate, which can be confirmed by Fig. 7(b). Figure 7(b) shows the local misorientation distribution for β phase in Figs. 6(a) and (b), which is associated with the geometrically necessary dislocations. The higher average local misorientation for β phase in Fig. 6(a) suggests a higher dislocation density/local strain [22] compared with that in Fig. 6(b). For the specimens compressed at a higher strain rate and

annealed, the solute diffusivity through the β matrix is accelerated during the early stage of annealing due to higher dislocation density/local strain [23,24], promoting penetration of β phase and leading to sharp grooves (Fig. 8(b)). As a result, significant globularization occurs (Fig. 8(c)) and the globularization fraction sharply increases during the first 20 min of annealing (Fig. 2(a)). Since more HABs develop after a larger height reduction, annealing the specimens with a 50% height reduction leads to a more rapid increase of globularization fraction during the first 20 min of annealing than that with a 20% height reduction (Fig. 2(a)). Moreover, the grooving may affect globularization during annealing for 20 min−1 h although the effect is not evident as that in the first 20 min annealing, especially for the specimens after a height reduction of 50%. As a result, most of α phases present a globular morphology, as shown in Fig. 4(b). However, for the as-compressed microstructure at a low strain rate, sufficient dynamic recovery occurs during compression [25], and the dislocation density/local strain is lower during the early stage of annealing (Fig. 9(a)). Therefore, the penetration of β phase is not sufficient in which shallow grooves occur (Fig. 9(b)), leading to insufficient pinch-off of α lamellae during the early stage of annealing (Fig. 9(c)), and the globularization fraction slowly increases during the first 20 min of annealing (Fig. 2(a)).

With the increase of annealing time, concurrent static recovery in β matrix largely decreases solute diffusivity through matrix [18], weakening thermal grooving by penetration of β phase. As a result, static globularization by grooving is weakened as annealing time increases. Meanwhile, termination migration and Ostwald ripening become more and more important in microstructure evolution [15], which can be rationalized by Figs. 2(b) and (c) where both length and thickness of α laths and/or grains increase during annealing for 1−4 h. For the specimens compressed at 1.0 s^{-1} and 50% height reduction and then annealed, most of α phases present a globular morphology after annealing for 1 h. With the increase of annealing time, a near globular microstructure occurs due to further coarsening by termination migration and Ostwald ripening, as shown in Fig. 8(d). Termination migration is usually accomplished by solute transport from edges of α laths to flat faces [11,15,18]. In the present study, large quantities of HABs remain for specimens compressed at 0.01 s^{-1} and annealed for 20 min (Fig. 6(b)). The HABs can also evolve from LABs during annealing [12]. The HABs can provide sufficient driving force for the solute diffusion from the intraphase α/α boundaries to the ends of α laths, sharpening the grooves and resulting in globular α grains. As seen from the inset in Fig. 5(b), a few globular α grains (indicated by the white arrows) occur. WEISS et al [12] also suggested that breaking up of α laths took place by the occurrence of HABs where penetration of β phase was limited. On the other hand, termination migration and Ostwald ripening coarsen α laths decrease the depth of grooves. As a result, the chain-like α grains occur (Fig. 9(d)). With further increase of annealing time, coalescence of adjacent α laths and/or grains occurs (Fig. 9(e)), contributing to the decrease in globularization (Fig. 2(a)) and sharp increase in both length (Fig. 2(b)) and thickness (Fig. 2(c)).

4 Conclusions

1) Microstructure evolution of Ti−5Al−2Sn−2Zr−4Mo−4Cr during annealing is highly related to strain rate and height reduction of predeformation, especially for strain rate. Compressing at a strain rate of 1.0 s^{-1} and annealing, the globularization fraction continuously increases with the increase of annealing time, and a larger height reduction promotes globularization during annealing. However, compressing at a strain rate of 0.01 s^{-1} and annealing, the globularization fraction decreases and the length of α laths and/or grains sharply increases during annealing for 2−4 h due to coalescence of adjacent α laths and/or grains.

2) The grooving process significantly affects microstructure evolution of Ti−5Al−2Sn−2Zr−4Mo−4Cr during the first 20 min of annealing. Annealing the specimens compressed at a strain rate of 1.0 s^{-1}, penetration of β phase is largely enhanced due to a higher dislocation density/local strain and globularization is more sufficient. However, the grooving process is limited after a strain rate of 0.01 s^{-1} and lots of HABs remain after the first 20 min of annealing. After prolonging annealing time, enhancing the effect of HABs, termination migration and Ostwald ripening, the chain-like α grains are developed.

3) A higher strain rate and larger height reduction are suggested before annealing so that a globular microstructure of Ti−5Al−2Sn−2Zr−4Mo−4Cr can be required.

References

[1] PENG Xiao-na, GUO Hong-zhen, SHI Zhi-feng, QIN Chun, ZHAO Zhang-long. Microstructure characterization and mechanical properties of TC4-DT titanium alloy after thermomechanical treatment [J]. Transactions of Nonferrous Metals Society of China, 2014, 24: 682−689.

[2] WANG Ke, LI Miao-quan. Characterization of discontinuous yielding phenomenon in isothermal compression of TC8 titanium alloy [J]. Transactions of Nonferrous Metals Society of China, 2016, 26: 1583−1588.

[3] BANERJEE D, WILLIAMS J C. Perspectives on titanium science and technology [J]. Acta Materialia, 2013, 61: 844−879.

[4] LÜTJERING G, WILLIAMS J C, GYSLER A. Microstructure and mechanical properties of titanium alloys [M]. Berlin: Springer, 2007.
[5] LUO Jiao, LI Lian, LI Miao-quan. Deformation behavior of Ti−5Al−2Sn−2Zr−4Mo−4Cr alloy with two initial microstructures during hot working [J]. Transactions of Nonferrous Metals Society of China, 2016, 26: 414−422.
[6] SHI Zhi-feng, GUO Hong-zhen, LIU Rui, WANG Xiao-chen, YAO Ze-kun. Microstructure and mechanical properties of TC21 titanium alloy by near-isothermal forging [J]. Transactions of Nonferrous Metals Society of China, 2015, 25: 72−79.
[7] WU Cheng-bao, YANG He, FAN Xiao-guang, SUN Zhi-chao. Dynamic globularization kinetics during hot working of TA15 titanium alloy with colony microstructure [J]. Transactions of Nonferrous Metals Society of China, 2011, 21: 1963−1969.
[8] DONG Xian-juan, LU Shi-qiang, ZHENG Hai-zhong. Dynamic spheroidization kinetics behavior of Ti−6.5Al−2Zr−1Mo−1V alloy with lamellar microstructure [J]. Transactions of Nonferrous Metals Society of China, 2016, 26: 1301−1309.
[9] LU Shi-qiang, LI Xin, WANG Ke-lu, DONG Xian-juan, FU M W. High temperature deformation behavior and optimization of hot compression process parameters in TC11 titanium alloy with coarse lamellar original microstructure [J]. Transactions of Nonferrous Metals Society of China, 2013, 23: 353−360.
[10] ZHAO Hui-jun, WANG Bao-yu, LIU Gang, YANG Lei, XIAO Wen-chao. Effect of vacuum annealing on microstructure and mechanical properties of TA15 titanium alloy sheets [J]. Transactions of Nonferrous Metals Society of China, 2015, 25: 1881−1888.
[11] SEMIATIN S L, FURRER D U. Fundamentals of modeling for metals processing [M]. OH: ASM International, 2009.
[12] WEISS I, FROES F H, EYLON D, WELSCH G E. Modification of alpha morphology in Ti−6Al−4V by thermomechanical processing [J]. Metallurgical Transactions A, 1986, 17: 1935−1947.
[13] SONG Hong-wu, ZHANG Shi-hong, CHENG Ming. Dynamic globularization kinetics during hot working of a two-phase titanium alloy with a colony alpha microstructure [J]. Journal of Alloys and Compounds, 2009, 480: 922−927.
[14] ROY S, MADHAVAN R, SUWAS S. Crystallographic texture and microstructure evolution during hot compression of Ti−6Al−4V−0.1B alloy in the (α+β)-regime [J]. Philosophical Magazine, 2014, 94: 358−380.
[15] STEFANSSON N, SEMIATIN S L. Mechanisms of globularization of Ti−6Al−4V during static heat treatment [J]. Metallurgical and Materials Transactions A, 2003, 34: 691−698.
[16] LI L, LI M Q, LUO J. Mechanism in the β phase evolution during hot deformation of Ti−5Al−2Sn−2Zr−4Mo−4Cr with a transformed microstructure [J]. Acta Materialia, 2015, 94: 36−45.
[17] LI L, LI M Q, LUO J. Flow softening mechanism of Ti−5Al−2Sn−2Zr−4Mo−4Cr with different initial microstructures at elevated temperature deformation [J]. Materials Science Engineering A, 2015, 628: 11−20.
[18] ZHEREBTSOV S, MURZINOVA M, SALISHCHEV G, SEMIATIN S L. Spheroidization of the lamellar microstructure in Ti−6Al−4V alloy during warm deformation and annealing [J]. Acta Materialia, 2011, 59: 4138−4150.
[19] MULLINS W W. Theory of thermal grooving [J]. Journal of Applied Physics, 1957, 28: 333−339.
[20] ZHEREBTSOV S, SALISHCHEV G, SEMIATIN S L. Loss of coherency of the alpha/beta interface boundary in titanium alloys during deformation [J]. Philosophical Magazine Letters, 2010, 90: 903−914.
[21] CABIBBO M, ZHEREBTSOV S, MIRONOV S, SALISHCHEV G. Loss of coherency and interphase α/β angular deviation from the Burgers orientation relationship in a Ti−6Al−4V alloy compressed at 800 °C [J]. Journal of Materials Science, 2013, 48: 1100−1110.
[22] SUN J L, TRIMBY P W, YAN F K, LIAO X Z, TAO N R, WANG J T. Shear banding in commercial pure titanium deformed by dynamic compression [J]. Acta Materialia, 2014, 79: 47−58.
[23] SEMIATIN S L, CORBETT M W, FAGIN P N, SALISHCHEV G A, LEE C S. Dynamic-coarsening behavior of an α/β titanium alloy [J]. Metallurgical and Materials Transactions A, 2006, 37: 1125−1136.
[24] PORTER D A, EASTERLING K E. Phase transformation in metals and alloys [M]. 2nd ed. London: Chapman & Hall, 1992.
[25] HUMPHREYS F J, HATHERLY M. Recrystallization and related annealing phenomena [M]. 2nd ed. Oxford: Elsevier, 2004.

预变形对 Ti−5Al−2Sn−2Zr−4Mo−4Cr 退火过程中球化的影响

李 莲，李淼泉

西北工业大学 材料学院，西安 710072

摘 要：研究 Ti−5Al−2Sn−2Zr−4Mo−4Cr 在退火过程中的显微组织演变。结果表明，合金在 810 °C、1.0 s^{-1} 条件下经 20%和 50%的压缩变形后再在 810 °C 进行退火处理，在前 20 min 退火过程中，β 相楔入形成热沟槽十分充分，球化率迅速增大；随退火时间延长，球化率继续增加。对经较大变形程度(50%)的合金进行 4 h 的退火处理获得了近似完全球化的组织。合金在 810 °C、0.01 s^{-1} 条件下经 50%变形后再在 810 °C 进行退火处理，在前 20 min 退火过程中，热沟槽作用并不明显，且保留了大量的大角度晶界。通过长时间退火，在大角度晶界、末端迁移和 Ostwald 熟化的共同作用下形成了项链状 α 相晶粒。因此，在 Ti−5Al−2Sn−2Zr−4Mo−4Cr 退火前应进行较高应变速率与较大程度的变形以获得等轴组织。

关键词：Ti−5Al−2Sn−2Zr−4Mo−4Cr 合金；退火；热沟槽；球化；大角度晶界

(Edited by Wei-ping CHEN)